

## Out-of-Equilibrium Kondo Effect in Double Quantum Dots

Ramón Aguado and David C. Langreth

Center for Materials Theory, Department of Physics and Astronomy, Rutgers University, Piscataway, New Jersey 08854-8019  
(Received 21 December 1999)

The out-of-equilibrium transport properties of a double quantum dot system in the Kondo regime are studied theoretically by means of a two-impurity Anderson Hamiltonian with interimpurity hopping. The Hamiltonian is solved by means of a nonequilibrium generalization of the slave-boson mean-field theory. It is demonstrated that measurements of the differential conductance  $dI/dV$ , for appropriate values of voltages and tunneling couplings, can give a direct observation of the coherent superposition between the many-body Kondo states of each dot. For large voltages and arbitrarily large interdot tunneling, there is a critical voltage above which the physical behavior of the system again resembles that of two decoupled quantum dots.

PACS numbers: 72.15.Qm, 73.20.Dx, 73.23.Hk

Recent experiments [1–3] have shown that new physics emerge when the transport properties of quantum dots (QD's) at temperatures ( $T$ ) below the Kondo temperature ( $T_K$ ) are studied [4]. QD's offer the intriguing possibility of a continuous tuning of the relevant parameters governing the Kondo effect [5] as well as the possibility of studying Kondo physics when the system is driven out of equilibrium in different ways [6]. These experimental breakthroughs have opened up a new way for the study of strongly correlated electrons in artificial systems. The Kondo anomaly appearing in the density of states (DOS) of the QD reflects the formation of a quantum-coherent many-body state. Motivated by the recent experimental advances in the study of double quantum dots (DQD) [7] it is thus interesting to study what happens when two QD's in the Kondo regime are coupled. Previous theoretical studies of this problem at equilibrium have focused on the competition between Kondo effect and antiferromagnetic coupling generated via superexchange [8,9] or via capacitive coupling between dots [10].

In this Letter we focus on the study of a DQD in the Kondo regime driven out of equilibrium by means of a dc voltage bias. There have hitherto been only a few attempts to study this problem [11] but a clear picture of the problem is yet missing. Following the recent work of Aono *et al.* [12] and Georges and Meir [8] we employ the slave-boson (SB) technique [13] in a mean-field approximation (MFA) and generalize it to a nonequilibrium situation. This MFA allows us to include nonperturbatively the interdot tunneling term (i.e., coherence between dots). The different physical regimes that appear as the ratio  $\tau_c = t_C/\Gamma$

changes ( $t_C$  is the interdot tunneling coupling and  $\Gamma$  is the single particle broadening coming from the coupling to the leads [14]) can be explored by measuring the nonlinear transport properties of the system. Our results can be summarized in Figs. 1 and 2: the differential conductance  $dI/dV$  of the DQD directly measures the transition (as  $\tau_c$  increases) from two isolated Kondo impurities to a coherent superposition of the many-body Kondo states of each dot, which form bonding and antibonding combinations. This coherent state which occurs for  $\tau_c > 1$  is reflected as a splitting of the zero-bias anomaly in the  $dI/dV$  curves. This splitting depends nontrivially on the voltage and on the many-body parameters of the problem. For large voltages, we find that there is a critical voltage above which the coherent configuration is unstable and the physical behavior of the system again resembles that of two decoupled QD's, i.e., two Kondo singularities pinned at each chemical potential, even for  $\tau_c > 1$ . This instability is reflected as a drastic drop of the current leading to singular regions of negative differential conductance (NDC).

*Model.*—In typical experiments,  $U_{\text{intradot}}, \Delta\epsilon \gg T$  ( $U_{\text{intradot}}$  is the strong on-site Coulomb interaction on each dot,  $\Delta\epsilon$  is the average level separation), which allows one to consider a single state in each QD [15]. We can model the DQD with a ( $N = 2$ ) fold degenerate two-impurity Anderson Hamiltonian with an extra term accounting for interdot tunneling. Each impurity is coupled to a different Fermi sea of chemical potential  $\mu_L$  and  $\mu_R$ , respectively. In the limit  $U_{\text{intradot}} \rightarrow \infty$  (on each QD) and  $U_{\text{interdot}} \rightarrow 0$  [16], the Hamiltonian may be written in terms of auxiliary SB operators [13] plus constraints:

$$H = \sum_{k_\alpha \in \{L,R\}, \sigma} \epsilon_{k_\alpha} c_{k_\alpha, \sigma}^\dagger c_{k_\alpha, \sigma} + \sum_{\alpha \in \{L,R\}, \sigma} \epsilon_{\alpha\sigma} f_{\alpha\sigma}^\dagger f_{\alpha\sigma} + \frac{t_C}{N} \sum_{\sigma} (f_{L\sigma}^\dagger b_L b_R^\dagger f_{R\sigma} + f_{R\sigma}^\dagger b_R b_L^\dagger f_{L\sigma}) + \frac{1}{\sqrt{N}} \sum_{k_\alpha \in \{L,R\}, \sigma} V_\alpha (c_{k_\alpha, \sigma}^\dagger b_\alpha^\dagger f_{\alpha\sigma} + f_{\alpha\sigma}^\dagger b_\alpha c_{k_\alpha, \sigma}) + \sum_{\alpha \in \{L,R\}} \lambda_\alpha \left( \sum_{\sigma} f_{\alpha\sigma}^\dagger f_{\alpha\sigma} + b_\alpha^\dagger b_\alpha - 1 \right). \quad (1)$$

$c_{k_\alpha, \sigma}^\dagger (c_{k_\alpha, \sigma})$  are the creation (annihilation) operators for electrons in the lead  $\alpha$ . To simplify the notation we consider henceforth that  $V_L = V_R = V_0$  and  $\epsilon_{L\sigma} = \epsilon_{R\sigma} =$

$\epsilon_0$  (i.e.,  $T_K$  is the same for both dots at equilibrium; the generalization to different  $T_K$ 's is straightforward). The

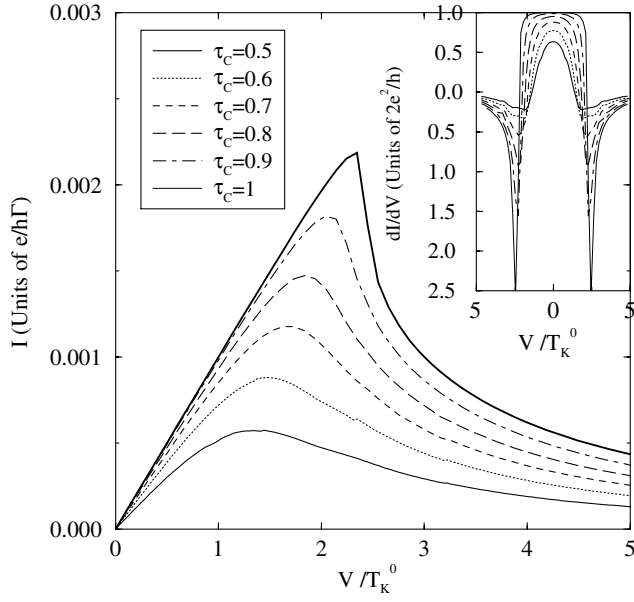


FIG. 1.  $I$ - $V$  curves for different values of  $\tau_c \leq 1$  and  $\epsilon_0 = -3.5$ . Inset:  $dI/dV$  curves for the same parameters.

even-odd symmetry is broken by the interdot coupling  $t_C$ . In the SB representation, the annihilation operator for electrons in the QD's,  $c_{\alpha\sigma}$  is decomposed into the SB operator  $b_\alpha^\dagger$  which creates an empty state and a pseudo-fermion operator  $f_{\alpha\sigma}$  which annihilates the singly occupied state with spin  $\sigma$  in the dot  $\alpha$ :  $c_{\alpha\sigma} \rightarrow b_\alpha^\dagger f_{\alpha\sigma}$  ( $c_{\alpha\sigma}^\dagger \rightarrow f_{\alpha\sigma}^\dagger b_\alpha$ ). In the last term of (1), the charge operator  $\hat{Q}_\alpha = \sum_\sigma f_{\alpha\sigma}^\dagger f_{\alpha\sigma} + b_\alpha^\dagger b_\alpha$  has been introduced. This term represents the constraint  $\hat{Q}_\alpha = 1$  in each dot with Lagrange multiplier  $\lambda_\alpha$ . This constraint prevents double occupancy in the limit  $U_{\text{intradot}} \rightarrow \infty$ .

*Solution.*—In the lowest order, we assume that the SB operator is a constant  $c$  number  $b_\alpha(t)/\sqrt{N} = \langle b_\alpha(t) \rangle / \sqrt{N} = \tilde{b}_\alpha$ , neglecting the fluctuations around the average  $\langle b_\alpha(t) \rangle$  of the SB. At  $T = 0$ , this MFA is correct for describing spin fluctuations (Kondo regime). Mixed-valence behavior (characterized by strong charge fluctuations) cannot be described by the MFA. This restricts our nonequilibrium calculation to low voltages  $V \ll \epsilon_0$ . Charge fluctuations can be included as thermal or quantum fluctuations ( $1/N$  corrections) [13,17]. By defining  $\tilde{V}_\alpha = V_0 \tilde{b}_\alpha$  and  $\tilde{t}_C = t_C \tilde{b}_L \tilde{b}_R$ , we obtain from the constraints and the equation of motion of the SB operators the self-consistent set of four equations with four unknowns ( $\tilde{b}_L, \tilde{b}_R, \lambda_L, \lambda_R$ ):

$$\begin{aligned} \tilde{b}_{L(R)}^2 + \frac{1}{N} \sum_\sigma \langle f_{L(R)\sigma}^\dagger f_{L(R)\sigma} \rangle &= \frac{1}{N}, \\ \frac{\tilde{V}_{L(R)}}{N} \sum_{k_{L(R),\sigma}} \langle c_{k_{L(R),\sigma}}^\dagger f_{L(R)\sigma} \rangle + \\ \frac{\tilde{t}_C}{N} \sum_\sigma \langle f_{R(L)\sigma}^\dagger f_{L(R)\sigma} \rangle + \lambda_{L(R)} \tilde{b}_{L(R)}^2 &= 0. \end{aligned} \quad (2)$$

In order to solve (2) we need to calculate the non-equilibrium distribution functions:  $G_{\alpha\sigma, k_{\alpha'}\sigma}^<(t-t') \equiv$

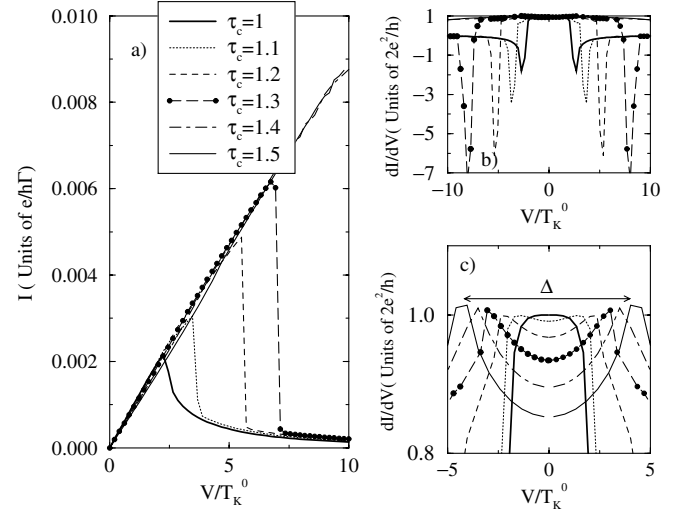


FIG. 2. (a)  $I$ - $V$  curves for different values of  $\tau_c \geq 1$  and  $\epsilon_0 = -3.5$ . (b)  $dI/dV$  curves for the same parameters. (c) Blowup (b). The arrow shows the splitting  $\Delta = 2\delta$  for  $\tau_c = 1.5$ .

$i\langle c_{k_{\alpha'}\sigma}^\dagger(t') f_{\alpha\sigma}(t) \rangle$  and  $G_{\alpha\sigma, \alpha'\sigma}^<(t-t') \equiv i\langle f_{\alpha'\sigma}^\dagger(t') \times f_{\alpha\sigma}(t) \rangle$ . They can be derived by applying the analytic continuation rules of Ref. [18] to the equation of motion of the time-ordered Green's function along a complex contour (Keldysh, Kadanoff-Baym, or a more general choice). This allows us to relate  $G_{\alpha\sigma, k_{\alpha'}\sigma}^<(t-t')$  with  $G_{\alpha\sigma, \alpha'\sigma}^<(t-t')$  and  $G_{\alpha\sigma, \alpha'\sigma}^r(t-t') \equiv -i\theta(t-t') \langle \{ f_{\alpha\sigma}(t), f_{\alpha'\sigma}^\dagger(t') \} \rangle$  and close the set of equations (2) in Fourier space:

$$\begin{aligned} \frac{\tilde{\Gamma}_{L(R)}}{\Gamma} - i \int \frac{d\epsilon}{2\pi} G_{L,L(R,R)}^<(\epsilon) &= \frac{1}{N}, \\ \frac{\tilde{\Gamma}_{L(R)}}{\Gamma} (\tilde{\epsilon}_{L(R)} - \epsilon_0) = i \int \frac{d\epsilon}{2\pi} G_{L,L(R,R)}^<(\epsilon) (\epsilon - \tilde{\epsilon}_{L(R)}), \end{aligned} \quad (3)$$

with  $\tilde{\epsilon}_\alpha = \epsilon_0 + \lambda_\alpha$  and  $\tilde{\Gamma}_\alpha = \tilde{b}_\alpha^2 \Gamma$ . For  $t_C = 0$ ,  $\tilde{\epsilon}_\alpha$  and  $\tilde{\Gamma}_\alpha$  give, respectively, the position and width of the Kondo peaks in the dot  $\alpha$  (at equilibrium, and in the Kondo regime,  $\sqrt{\tilde{\epsilon}_\alpha^2 + \tilde{\Gamma}_\alpha^2} \equiv T_K^0 = De^{-\pi|\epsilon_0|/\Gamma}$ ) [5]. The distribution functions in the QD's are  $G_{L,L(R,R)}^<(\epsilon) = \frac{2i(\tilde{\Gamma}_{L(R)} f_{L(R)}(\epsilon) [(\epsilon - \tilde{\epsilon}_{R(L)})^2 + \tilde{\Gamma}_{R(L)}^2] + \tilde{\Gamma}_{R(L)} f_{R(L)}(\epsilon) \tilde{t}_C^2)}{[(\epsilon - \tilde{\epsilon}_L + i\tilde{\Gamma}_L)(\epsilon - \tilde{\epsilon}_R + i\tilde{\Gamma}_R) - \tilde{t}_C^2][(\epsilon - \tilde{\epsilon}_L - i\tilde{\Gamma}_L)(\epsilon - \tilde{\epsilon}_R - i\tilde{\Gamma}_R) - \tilde{t}_C^2]}$ , where  $f_{L(R)}(\epsilon)$  is the Fermi-Dirac function in the left (right) lead. Note that the presence of  $\tilde{t}_C^2$  in the denominators indicates that the interdot tunneling enters nonperturbatively in the calculations and, then, coherent effects between dots are fully included. Because of the interdot tunneling, the Kondo singularities of each dot at  $\tilde{\epsilon}_L$  and  $\tilde{\epsilon}_R$  combine into coherent superpositions at  $\epsilon_\pm = \frac{1}{2}[(\tilde{\epsilon}_L + \tilde{\epsilon}_R) \pm \sqrt{(\tilde{\epsilon}_L - \tilde{\epsilon}_R)^2 + 4\tilde{t}_C^2}]$ . Of course, at equilibrium  $\tilde{b}_L = \tilde{b}_R = \tilde{b}$ ,  $\lambda_L = \lambda_R = \lambda$ , we recover the results of Refs. [8,12]. Note that the formation of coherent superpositions of the Kondo singularity is not trivially related with its single particle counterpart (formation of bonding and antibonding states at  $\epsilon_0 \pm t_C$ ).

Let us focus for simplicity on the equilibrium case ( $\tilde{\epsilon}_L = \tilde{\epsilon}_R$ ); the splitting is given by  $\delta \equiv \epsilon_+ - \epsilon_- = 2\tilde{t}_C$  which is a *many-body* parameter (given by the strong renormalization of the interdot tunneling due to the Kondo effect).  $\delta$  depends *nonlinearly* on the single particle splitting  $\delta_0 = 2t_C$  (see Inset of Fig. 3a). In the Kondo limit,  $\{[(\tilde{\epsilon} + \tilde{t}_C)^2 + \tilde{\Gamma}^2][(\tilde{\epsilon} - \tilde{t}_C)^2 + \tilde{\Gamma}^2]\}^{1/4} = T_K^0 e^{\pi t_C/\Gamma} (\tilde{\Gamma}/\Gamma^{-1/2})$ . From the solution of Eq. (3) we obtain the current  $I = \frac{2e}{\hbar} \text{Re}\{\sum_{k_L, \sigma} \tilde{V}_L G_{L\sigma, k_L, \sigma}^<(t, t)\}$  and DOS in each QD:  $\rho_{L(R)}(\epsilon) = -\frac{1}{\pi} \text{Im}\left\{\frac{b_{L(R)}^2(\epsilon - \tilde{\epsilon}_{R(L)} + i\tilde{\Gamma}_{R(L)})}{[(\epsilon - \tilde{\epsilon}_L + i\tilde{\Gamma}_L)(\epsilon - \tilde{\epsilon}_R + i\tilde{\Gamma}_R) - \tilde{t}_C^2]}\right\}$ .

**Results.**— We solve numerically (for  $T = 0$ ) the set of nonlinear equations (3) for different voltages  $\mu_L = V/2$  and  $\mu_R = -V/2$ ,  $\epsilon_0 = -3.5$ ,  $D = 60$  (Kondo regime with  $T_K^0 \approx 10^{-3}$ ), and different values for the rest of the parameters (all energies in units of  $\Gamma$ ). Depending on the ratio  $\tau_c = t_C/\Gamma$ , we find two different physical scenarios for  $\tau_c < 1$  and  $\tau_c \geq 1$ .

In Fig. 1 we plot the  $I$ - $V$  curves (for clarity, we show only the  $V \geq 0$  region) for  $\tau_c \leq 1$ . The two main features of these curves are: (i) an increase of the linear conductance  $\mathcal{G} = dI/dV|_{V=0}$  as  $\tau_c$  increases and (ii) a saturation, followed by a drop, of the current for large voltages. This drop sharpens as  $\tau_c \rightarrow 1$ . These features are more pronounced in a plot of the  $dI/dV$  (inset of Fig. 1). As  $\tau_c$  increases, the zero-bias anomaly (originating from the Kondo resonance in the DOS of the dots) becomes broader and broader until it saturates into a flat region of value  $2e^2/h$  (unitary limit) for  $\tau_c = 1$ . The reduction of the current at larger  $V$  is reflected as NDC regions in the  $dI/dV$  curves. For  $\tau_c = 1$  this NDC becomes singular. For  $\tau_c > 1$ , and contrary to the previous case,  $\mathcal{G}$  *decreases* for increasing values of  $\tau_c$  (Fig. 2a). This reduction of  $\mathcal{G}$  can be attributed to the formation of the

coherent superposition of the Kondo states. This can be clearly seen as a splitting  $\Delta = 2\delta$  in the  $dI/dV$  curves (Fig. 2c): By increasing  $\tau_c$ , the zero-bias conductance decreases, whereas two maxima at  $\pm V_{\text{peak}}$  show up (the arrow shows the splitting  $\Delta = 2V_{\text{peak}}$  for the maximum value of  $\tau_c$  in the figure). Figure 2c demonstrates that the  $dI/dV$  curves of a DQD in the Kondo regime directly measure the *coherent* combination between the two many-body states in the QD's. For larger voltages, the sharp drop of the current (Fig. 2a) reflects as strong NDC singularities as in the  $dI/dV$  curves (Fig. 2b).

The position of these singularities moves towards higher  $|V|$  as  $\tau_c$  increases. In order to explain the results of Figs. 1 and 2, we plot in Fig. 3a  $\epsilon_{\pm}$  as a function of  $V \geq 0$  for different values of  $\tau_c$ . For  $\tau_c = 0$  (thick solid line), this corresponds to a plot of  $\tilde{\epsilon}_L$  and  $\tilde{\epsilon}_R$  (i.e., the positions of the Kondo resonances for the decoupled QD's) as a function of  $V$ . We find, as expected, that each Kondo resonance is pinned at the chemical potential of its own lead,  $\tilde{\epsilon}_L = \mu_L = V/2$  and  $\tilde{\epsilon}_R = \mu_R = -V/2$ . As the interdot coupling is turned on, the voltage dependence becomes strongly nonlinear. For low  $V$ , the curves for  $\tau_c \neq 0$  do not coincide with the curves for  $\tau_c = 0$  (i.e.,  $\mu_{L/R}$ ). This situation, however, changes as we increase  $V$ ; the level positions  $\epsilon_{\pm}$  converge towards the chemical potentials  $\mu_{L/R}$  in a nontrivial way.

The voltage  $V$  for which  $\epsilon^+ - \epsilon^-$  coincides with the chemical potential difference  $V$  gives the position of the peak in the positive side of the  $dI/dV$  (Fig. 2c). This voltage is the solution of the equation  $\delta(V_{\text{peak}}) = V_{\text{peak}}$ , where  $\delta(V) \equiv \sqrt{(\tilde{\epsilon}_L - \tilde{\epsilon}_R)^2 + 4\tilde{t}_C^2}$ , with  $\tilde{\epsilon}_{L/R}$  given by Eq. (3). Note the implicit (and nontrivial) voltage dependence of  $\delta(V)$ .  $\tilde{\Gamma}_L$ ,  $\tilde{\Gamma}_R$ , and  $\tilde{t}_C$  follow a similar behavior as a function of  $V$  (Figs. 3b–3d). For  $V \geq V_{\text{peak}}$ , we find numerically that  $\delta(V) \approx V$  a relationship that becomes asymptotically exact as  $V \rightarrow \infty$ . The equation  $\delta(V) = V$  has stable solutions  $\tilde{t}_C \neq 0$  for  $[\frac{(\tilde{\epsilon}_L - \tilde{\epsilon}_R)}{V}]^2 < 1$ , while, for  $[\frac{(\tilde{\epsilon}_L - \tilde{\epsilon}_R)}{V}]^2 > 1$ , the only stable solution is  $\tilde{t}_C = 0$ , corresponding to current  $I = 0$ . We denote the crossover voltage where  $[\frac{(\tilde{\epsilon}_L - \tilde{\epsilon}_R)}{V}]^2 = 1$  by  $V^*$ . For finite voltages  $V > V_{\text{peak}}$ , on the other hand, the relation  $\delta(V) = V$  is only approximate, so that, at the crossover  $\approx V^*$ , the quantity  $\tilde{t}_C$  and hence  $I$  drop to a much smaller, but still finite, value instead. Nevertheless, the crossover at  $V \approx V^*$  still indicates the beginning of the NDC region.

To illustrate this, we plot in Fig. 4 the left and right QD's DOS for  $\tau_c = 1$ . At equilibrium ( $V = 0$ ), the Kondo singularity at  $\epsilon = 0$  splits into the  $\epsilon_{\pm}$  combinations. For  $V/T_K^0 = 2$  the coherence is still preserved but the physical picture utterly changes for higher voltages ( $V/T_K^0 = 4$  and  $V/T_K^0 = 6$ ). In this case, the previous configuration is no longer stable, the coherence between dots is lost ( $\tilde{t}_C \rightarrow 0$ ), the dots are almost decoupled, and the Kondo resonances in each dot are pinned again at their own chemical potential: the weight of the left (right) DOS at  $\epsilon = \mu_{R(L)}$  is almost zero (even though  $\tau_c = 1$ ).

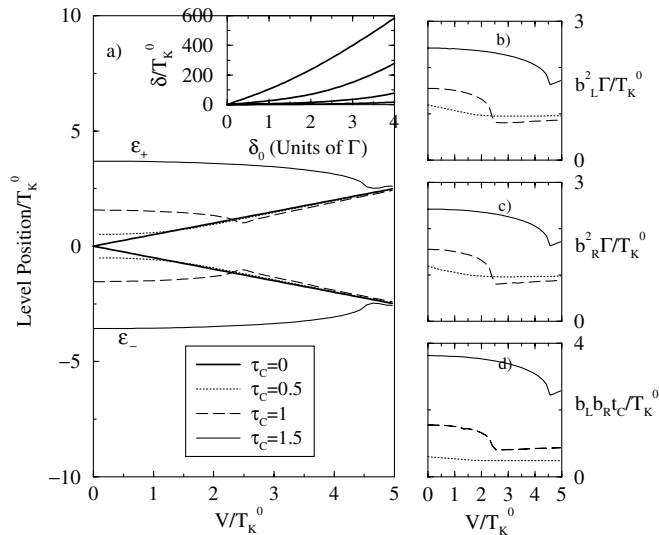


FIG. 3. (a)  $\epsilon_{\pm}$  vs  $V$  for different values of  $\tau_c$  ( $\epsilon_0 = -3.5$ ). Inset: Many-body splitting ( $\delta$ ) as a function of the single particle splitting ( $\delta_0$ ) for  $V = 0$  and  $\epsilon_0 = -2.0, -2.5, -3.0, -3.5$  (from top to bottom). (b)  $\tilde{\Gamma}_L$  vs  $V$ . (c)  $\tilde{\Gamma}_R$  vs  $V$ . (d)  $\tilde{t}_C$  vs  $V$ .

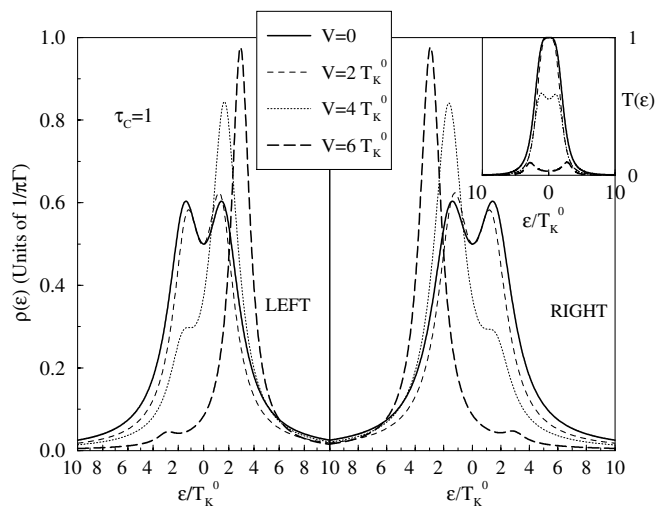


FIG. 4. DOS for the left and right dot for  $\tau_c = 1$  and different voltages ( $\epsilon_0 = -3.5$ ). Inset: transmission probability of the DQD for the same parameters.

This instability resembles that of the SB at  $T \neq 0$  in the single-impurity Anderson Hamiltonian [17,19]. In the MFA the SB behaves as the order parameter associated with the conservation of  $Q$ . When  $\tilde{b} \neq 0$  the gauge symmetry  $b \rightarrow be^{i\theta}$ ,  $f \rightarrow fe^{i\theta}$  associated with charge conservation is broken, and the MFA has two phases  $\tilde{b} \neq 0$  and  $\tilde{b} = 0$  separated by a second order phase transition. It is important to point out that the fluctuations do not destroy completely this  $\tilde{b} \rightarrow 0$  behavior (the SB fluctuations develop power law behavior, replacing the transition by a smooth crossover). We speculate that in our problem this zero-temperature transition at finite  $V$  may also be robust against fluctuations, but  $1/N$  corrections are needed to substantiate this argument. Work in this direction is in progress.

In conclusion, we have demonstrated that the nonlinear transport properties ( $dI/dV$ ) of a DQD in the Kondo regime directly measure the transition (as  $t_C$  increases) from two isolated Kondo impurities to a coherent bonding and antibonding superposition of the many-body Kondo states of each dot. While for  $t_C < \Gamma$  the conductance maximum is at  $V = 0$ , for  $t_C > \Gamma$  the transport is optimized for a finite  $V$  matching the splitting between these two bonding and antibonding states. For large voltages (and  $t_C \geq \Gamma$ ) there is a critical voltage above which the coherent superposition is unstable and the physical behavior of the system again resembles that of two decoupled QD's. This leads to a strong reduction of the current and singular regions of negative differential conductance. Concerning the observability of these effects, in our MFA the maximum value of  $\delta$  ranges from  $\delta \approx 20T_K^0 - 500T_K^0$  (inset of Fig. 3a) giving, for the experiment of Ref. [1]

( $\Gamma \sim 150 \mu\text{eV}$ ),  $\delta \sim 3-75 \mu\text{eV}$  (30-750 mK) which is within the resolution limits of present day techniques.

This work was supported by the NSF Grant No. DMR 97-08499, DOE Grant No. DE-FG02-99ER45970, and by the MEC of Spain Grant No. PF 98-07497938.

- [1] D. Goldhaber-Gordon *et al.*, Nature (London) **391**, 156 (1998); Phys. Rev. Lett. **81**, 5225 (1998).
- [2] S.M. Cronenwett *et al.*, Science **281**, 540 (1998).
- [3] J. Schmid *et al.*, Physica (Amsterdam) **256B-258B**, 182 (1998).
- [4] T.K. Ng and P.A. Lee, Phys. Rev. Lett. **61**, 1768 (1988); L.I. Glazman and M.E. Raikh, JETP Lett. **47**, 452 (1988); A. Kawabata, J. Phys. Soc. Jpn. **60**, 3222 (1991).
- [5] A.C. Hewson *The Kondo Problem to Heavy Fermions* (Cambridge University Press, Cambridge, UK, 1993).
- [6] S. Hershfield *et al.*, Phys. Rev. Lett. **67**, 3720 (1991); Y. Meir *et al.*, *ibid.* **70**, 2601 (1993); A.L. Yeyati *et al.*, *ibid.* **71**, 2991 (1993); M.H. Hettler and H. Schoeller, *ibid.* **74**, 4907 (1995); T.K. Ng, *ibid.* **76**, 487 (1996); A. Schiller and S. Hershfield, *ibid.* **77**, 1821 (1996); R. López *et al.*, *ibid.* **81**, 4688 (1998); Y. Goldin and Y. Avishai, *ibid.* **81**, 5394 (1998); A. Kaminski *et al.*, *ibid.* **83**, 384 (1999); P. Nordlander *et al.*, Phys. Rev. B **61**, 2146 (2000); M. Plihal *et al.*, Phys. Rev. B **61**, R13341 (2000).
- [7] T.H. Oosterkamp *et al.*, Nature (London) **395**, 873 (1998); T. Fujisawa *et al.*, Science **282**, 932 (1998).
- [8] A. Georges and Y. Meir, Phys. Rev. Lett. **82**, 3508 (1999).
- [9] C.A. Büsser *et al.*, cond-mat/9912019; W. Izumida and O. Sakai, cond-mat/9912296.
- [10] N. Andrei *et al.*, Phys. Rev. B. **60**, R5125 (1999).
- [11] T. Ivanov, Europhys. Lett. **40**, 183 (1997); T. Pohjola *et al.*, Europhys. Lett. **40**, 189 (1997).
- [12] T. Aono *et al.*, J. Phys. Soc. Jpn. **67**, 1860 (1998).
- [13] P. Coleman, Phys. Rev. B **29**, 3035 (1984).
- [14]  $\Gamma(\epsilon) = \pi \sum_{k_\alpha} |V_0|^2 \delta(\epsilon - \epsilon_{k_\alpha})$ . We take  $\Gamma \equiv \Gamma(\epsilon_F) - D \leq \epsilon \leq D$  ( $D$  serves as a cutoff in the calculations).
- [15] For  $\Gamma \sim \Delta\epsilon$  the effect of multiple levels has to be taken into account. For single QD's, see A.L. Yeyati *et al.*, Phys. Rev. Lett. **83**, 600 (1999).
- [16] The neglect of  $U_{\text{interdot}}$  corresponds to the experimentally accessible limit of small interdot capacitance as compared with the capacitances of each QD to the gates, and implies a vanishing interdot antiferromagnetic coupling from this source. The antiferromagnetic coupling due to superexchange also vanishes in the model, because  $U_{\text{intradot}} \rightarrow \infty$ .
- [17] N. Read, J. Phys. C **18**, 2651 (1985); P. Coleman, J. Magn. Magn. Mater. **47**, 323 (1985).
- [18] D.C. Langreth, in *Linear and Nonlinear Electron Transport in Solids*, edited by J. T. Devreese and V.E. Van Daren, Nato ASI, Ser. B, Vol. 17 (Plenum, New York, 1976).
- [19] In the nonequilibrium case ( $T = 0$ ) it also appears at a voltage  $\frac{V^*}{2T_K^0} = 1$ . Piers Coleman (private communication).